

Room temperature sub-diffraction-limited plasmon laser by total internal reflection

Ren-Min Ma^{1*}, Rupert F. Oulton^{1*}, Volker J. Sorger¹, Guy Bartal¹ & Xiang Zhang^{1,2†}

¹*NSF Nanoscale Science and Engineering Centre, 3112 Etcheverry Hall, University of California, Berkeley, California 94720, USA.*

²*Materials Sciences Division, Lawrence Berkeley National Laboratory, 1 Cyclotron Road, Berkeley, California 94720, USA*

**These authors contributed equally to this work. †e-mail: xiang@berkeley.edu.*

Plasmon lasers are a new class of coherent optical amplifiers that generate and sustain light well below its diffraction limit [1-4]. Their intense, coherent and confined optical fields can enhance significantly light-matter interactions and bring fundamentally new capabilities to bio-sensing, data storage, photolithography and optical communications [5-11]. However, metallic plasmon laser cavities generally exhibit both high metal and radiation losses, limiting the operation of plasmon lasers to cryogenic temperatures, where sufficient gain can be attained. Here, we present room temperature semiconductor sub-diffraction limited laser by adopting total internal reflection of surface plasmons to mitigate the radiation loss, while utilizing hybrid semiconductor-insulator-metal nano-squares for strong confinement with low metal loss. High cavity quality factors, approaching 100, along with strong $\lambda/20$ mode confinement lead to enhancements of spontaneous emission rate by up to 18 times. By controlling the structural geometry we reduce the number of cavity modes to achieve single mode lasing.

Lasers are ideal for optical communications, information storage, accurate metrologies and sensitive spectroscopies as they present the means to deliver powerful, coherent and directional high frequency electromagnetic energy. However, the diffraction limit of light imposes fundamental constraints on how compact such photonic devices can be and their potential for integration with electronic circuits, which are orders of magnitude smaller.

While recent efforts in photonic crystal, whispering gallery and metal-coated photonic cavities have succeeded in confining light to less than the vacuum wavelength, they remain limited by diffraction [12-16]. On the other hand, surface plasmon polaritons (SPPs) [17], the collective electronic oscillations of metal-dielectric interfaces, show great promise for an exciting new class of light source capable of reconciling photonic and electronic length scales. Furthermore, SPPs are capable of extremely strong confinement in one or two dimensions [2, 4, 18, 19], enabling *plasmon lasers* to deliver intense, coherent and directional optical energy well below the diffraction barrier. Such lasers can drastically accelerate the scalability of photonics to catch up with Moore's law for electronics and will naturally introduce new functionalities and applications.

Notwithstanding the growing body of work on metal-based lasers, the demonstration of sub-diffraction limited semiconductor plasmon lasers operating at room temperature remains a major hurdle owing to the problem of mitigating both the high absorptive loss of metals and the low cavity feedback of propagating surface plasmons in small metallic structures. This has restricted such lasers to working at cryogenic temperatures in order to attain sufficient gain [2, 4]. Recent efforts in semiconductor plasmon lasers were only able to partially tackle these obstacles and the design stratagems remain mutually exclusive: improved feedback was obtained in devices capped in metal at the expense of high metal loss resulting in limited mode confinement [2]; whereas nanowire lasers on planar metal substrates achieved reduced metal loss but had limited feedback that required cavity lengths much longer than the wavelength [4]. Room temperature plasmon laser operation below the diffraction limit demands effective cavity feedback, low metal loss and high gain; all within a single nano-scale device.

Here, we report the first realization of semiconductor plasmon laser operating at room temperature with $\lambda/20$ optical confinement. A 45 nm thick Cadmium Sulphide (CdS) nano-square atop a Silver surface separated by a 5 nm thick Magnesium Fluoride gap layer provides the sub-wavelength mode confinement and low metal loss [20].

Surprisingly, although the high-index material is only 45 nm thick, the surface plasmons of this system carry high momentum, even higher than light waves in bulk CdS or plasmonic nanowire lasers [4]. This leads to strong feedback by total internal reflection of surface plasmons at the cavity boundaries.

Figures 1a and 1b show a schematic of the room temperature plasmon laser and a SEM micrograph of the 45 nm thick, 1 μm length square plasmon laser sitting atop a Silver substrate with a 5 nm MgF_2 gap. The close proximity of the high permittivity CdS square and silver surface allows modes of the CdS square to hybridize with SPPs of the metal-dielectric interface, leading to strong confinement of light in the gap region (Fig. 1c) with relatively low metal loss [20]. The coupling is extremely strong and causes a dramatic increase in the momentum with respect to the modes of the CdS square alone (blue arrow in Fig. 1d). Since the dominant magnetic field component of the waves is always parallel to the metal surface we call these transverse magnetic (TM) waves [21]. On the other hand, waves with dominant electric field parallel to the metal surface (transverse electric, or TE) cannot hybridize with SPPs. Consequently, they become increasingly de-localized as the gap size decreases and are effectively pushed away from the metal surface (Fig. 1c) with a corresponding decrease in momentum with respect to TE waves of the CdS square alone (red arrow in Fig. 1d). While both wave polarizations are free to propagate in the plane, only TM waves have sufficient momentum to undergo total internal reflection and achieve the necessary feedback for lasing as shown in Fig 1e [22, 23]. Although CdS squares thicker than about 60 nm can support TE waves with sufficient momentum to undergo total internal reflection, they are scattered out of the plane more effectively than TM waves since they are delocalized from the metal surface. While long lived eigenmodes of square cavities are achievable [24], the finite size of the cavity leads to imperfect internal reflection causing in-plane scattering of surface plasmon waves and volume scattering of radiation waves, which we use to measure the response of the plasmon laser (see supplementary information).

The feedback mechanism of totally internally reflected SPPs is extremely effective as shown by the well-pronounced cavity modes in the spontaneous emission spectrum below threshold (see supplementary information) in fig. 2a. The Q factors of the two apparent modes are 97 and 38 at the resonant wavelengths of 495.5 nm and 508.4 nm, respectively. We have identified these as plasmonic total internal reflection modes using a numerical model (see supplementary material). While the Q of the 495.5 nm resonance is close to numerical predictions, the other Q value is an underestimate because that resonance is composed of several modes that are too close to be resolved. For larger pump intensities, multiple cavity modes appear with orders of magnitude higher coherence than the underlying spontaneous emission, as shown in Fig. 2b. The emission spectrum is completely dominated by these high coherence peaks when collecting the light at large collection angles. This is a signature of the plasmonic cavity modes, which preferentially scatter into large angles to conserve their in-plane momentum (see supplementary information). The nonlinear response of the integrated output power with pump intensity confirms the observation of laser oscillation well above threshold (inset of Fig. 2). This laser can be considered to be a SPASER (Surface Plasmons Amplified by Stimulated Emission of Radiation) as it was originally introduced in Ref. 1, since it generates plasmonic cavity eigenmodes and only emits light to the far-field as a side effect of scattering.

The current device exhibits multiple laser peaks attributed to the number of available modes in the square cavity configuration (see supplementary information). However, we have also observed single mode plasmon lasing in irregularly shaped devices with lower symmetry where only a limited number of modes can undergo total internal reflection. Figure 3 shows the spectrum and power response of a single mode room temperature plasmon laser along with a SEM micrograph of the device with 75 nm thick, 1.1 μm length in Fig 3b. Lasing in such ultrathin devices is viable solely due to the plasmonic confinement and strong total internal reflection feedback. This was verified from control

samples; consisting of similar CdS squares on quartz substrates, none exhibited laser action due to the lack of both mode confinement and cavity feedback.

The intense fields that are generated and sustained in the gap region (Fig. 1c) make such lasers highly useful for investigating light-matter interactions. Namely, an emitter placed in this gap region is expected to interact strongly with the laser light. Such light-matter interaction enhancements are also observable to a lesser extent in the CdS gain medium; under weak pumping, the CdS band edge transitions of this plasmon laser (device shown in Fig. 1b) show a spontaneous emission lifetime reduced by a factor of 14 (Fig. 4a). The Purcell effect [25] is apparent in all the laser devices measured as shown in Fig. 4b. We note that in this work we sacrifice the lateral confinement, achievable in plasmonic nanowire lasers, [4] and use surface plasmon total internal reflection to realize a cavity with strong feedback. It is this combination of both high cavity quality factors (Q) and strong mode confinement that leads to Purcell factors as large as 18 in smaller devices. On the other hand, for devices larger than the surface plasmon propagation length, the cavity feedback no longer plays a role and an average 2-fold reduction in lifetime is obtained due to the strong confinement of SPPs alone. A theoretical formula describing the observed lifetime reduction is shown in Fig 4b and predicts SPP losses of $6,323 \text{ cm}^{-1}$, in good agreement with the numerical estimate (see Methods). We note that this plasmon loss can be compensated by gain available in CdS [26]. Since the electric field intensities in the gap region are 5 times stronger than in the CdS, we anticipate Purcell factors as high as 90 for light-matter interactions within the gap. Despite sub-diffraction limited confinement in only one dimension, this value is even higher than the highest simulated Purcell factors of 60 for the recently reported metal-coated photonic cavities [14-16].

We have demonstrated room temperature semiconductor plasmon lasers with strong mode confinement, which are also much smaller than the diffraction limit. The mode is generated inside a nanoscopic gap layer of 5 nanometers and remains bound by strong feedback arising from total internal reflection of surface plasmons. The small mode size

and high quality factor gives rise to a strong Purcell effect, resulting in up to an 18 fold enhancement of the natural spontaneous emission rate of CdS band-edge transitions. This indicates that these sub-diffraction limited laser modes have the potential to enhance light-matter interactions. Room temperature plasmon lasers enable new possibilities in applications such as single molecular sensing, ultra-high density data storage, nano lithography and optical communications.

References

1. Bergman, D. J. & Stockman, M. I. Surface Plasmon Amplification by Stimulated Emission of Radiation: Quantum Generation of Coherent Surface Plasmons in Nanosystems. *Physical Review Letters* **90**, 027402 (2003)
2. Hill, M. T. *et al.* Lasing in metal-insulator-metal sub-wavelength plasmonic waveguides. *Optics Express* **17**, 11107-11112 (2009).
3. Noginov, M. A. *et al.* Demonstration of a spaser-based nanolaser. *Nature* **460**, 1110-1113 (2009).
4. Oulton, R. F. *et al.* Plasmon lasers at deep subwavelength scale. *Nature*, **461**, 629-632 (2009).
5. Schuller, J. A. Barnard, E. S., Cai, W., Jun, Y. C., White, J. S. & Brongersma, M. L. Plasmonics for extreme light concentration and manipulation. *Nature Materials* **9**, 193-204 (2010)
6. Gramotnev, D. K., & Bozhevolnyi, S. I. Plasmonics beyond the diffraction limit. *Nature Photonics* **4**, 83-91 (2010)

7. Anker, J. N., Hall, W. P., Lyandres, O., Shah, N. C., Zhao, J. & Van Duyne, R. P. Biosensing with plasmonic nanosensors. *Nature Materials* **7**, 442-453 (2008).
8. Dionne, J. A., Diest, K., Sweatlock, L. A. & Atwater, H. A. PlasMOSor: A Metal-Oxide-Si Field Effect Plasmonic Modulator. *Nano Letters* **9**, 897-902 (2009)
9. Zijlstra, P., Chon, J. W. M. & Gu, M. Five-dimensional optical recording mediated by surface plasmons in gold nanorods. *Nature* **459**, 410–413 (2009).
10. Challener, W. A. *et al.* Heat-assisted magnetic recording by a near-field transducer with efficient optical energy transfer. *Nature Photonics* **3**, 220-224 (2009).
11. Stipe, B. C. *et al.* Magnetic recording at 1.5 Pb m^{-2} using an integrated plasmonic antenna. *Nature Photonics* **4**, 484-488 (2010) .
12. Altug, H., Englund, Dirk. & Vuckovic, Jelena. Ultrafast photonic crystal nanocavity laser. *Nature Physics* **2**, 484-488 (2006).
13. Song, Q., Cao, H., Ho, S. T. & Solomon, G. S. Near-IR subwavelength microdisk lasers. *Appl. Phys. Lett.* **94**, 061109 (2009).
14. Hill, M. T. *et al.* Lasing in metallic-coated nanocavities. *Nature Photonics* **1**, 589–594 (2007).
15. Nezhad, M. P. *et al.* Room-temperature subwavelength metallo-dielectric lasers. *Nature Photonics* **4**, 395-399 (2010).
16. Yu, K., Lakhani, A. & Wu, M. C. Subwavelength metal-optic semiconductor nanopatch lasers. *Opt. Express* **18**, 8790–8799 (2010).

17. Maier, S. A. *Plasmonics: fundamentals and applications* (Springer, 2007)
18. Akimov, A. V. *et al.* Generation of single optical plasmons in metallic nanowires coupled to quantum dots. *Nature* **450**, 402–406 (2007).
19. Kolesov, R. *et al.* Wave–particle duality of single surface plasmon polaritons. *Nature Physics* **5**, 470–474 (2009).
20. Oulton, R. F., Sorger, V. J., Genov, D. A., Pile, D. F. P. & Zhang, X. A hybrid plasmonic waveguide for subwavelength confinement and long-range propagation. *Nature Photonics* **2**, 496–500 (2008).
21. The convention in this letter defers from the TM wave definition with respect to the dielectric-air interface where the total internal reflection takes place
22. Poon, A. W., Courvoisier, F. & Chang, R. K. Multimode resonances in square-shaped optical microcavities. *Optics Letters* **26**, 632–634 (2001)
23. Huang, Y.-Z. Chen, Q. Guo, W.-H. & Yu, L.-J. Experimental observation of resonant modes in GaInAsP microsquares resonators. *IEEE Photonics Technology Letters* **17**, 2589–2591 (2005).
24. Wiersig, J. Formation of long-lived, scarlike modes near avoided resonance crossings in optical microcavities. *Physical Review Letters* **97**, 253901 (2006).
25. Purcell, E. M. Spontaneous emission probabilities at radio frequencies. *Physical Review* **69**, 681 (1946).

26. Ninomiya, S. & Adachi, S. Optical properties of wurtzite CdS. *J. Appl. Phys.* **78**, 1193-1190 (1995).

27. Ma, R.-M. Dai, L. & G.-G. Qin, High-Performance Nano-Schottky Diodes and Nano-MESFETs Made on Single CdS Nanobelts. *Nano Letters* **7**, 868-873 (2007).

Acknowledgements

The authors thank X. B. Yin for valuable discussions. We acknowledge financial support from the US Air Force Office of Scientific Research (AFOSR) MURI program under grant no. FA9550-04-1-0434 and by the National Science Foundation Nano-scale Science and Engineering Center (NSF-NSEC) under award no. CMMI-0751621.

Author contributions

R.M.M., R.F.O. and X.Z. developed the device concept and design. R.M.M., R.F.O. and V.J.S. performed the experiments. R.F.O. and R.M.M. conducted theoretical simulations. R.M.M., R.F.O., G.B. and X.Z. discussed the results and wrote the manuscript.

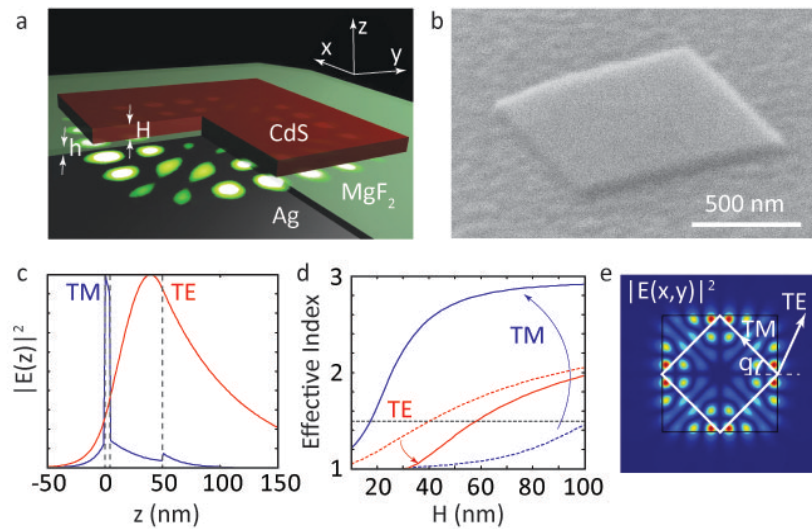


Figure 1 The room temperature plasmon laser. **a** Schematic of the room temperature plasmon laser showing a thin CdS square atop a Silver substrate separated by a 5nm MgF₂ gap where the most intense electric fields of the device reside. **b** SEM Micrograph of the 45 nm thick, 1 μm length CdS square plasmon laser studied in this letter. **c** The electric field intensity distribution of the two modes of the system along the z direction. While TM modes are localized in the gap layer, TE modes are delocalized from the metal surface. **d** The effective index of TM and TE waves with (solid line) and without (dashed line) the metal substrate. TM waves strongly hybridize with SPPs resulting in the strong confinement within the gap region (blue line in **c**) accompanied by a dramatic increase in momentum (blue line in **d**) with respect to TM waves of the CdS square alone (blue dashed line in **d**). However, the delocalized TE waves (red line in **c**) show decreased momentum (red line in **d**) with respect to TE waves of the CdS square alone (red dashed line in **d**). **e** Electric field intensity distribution of a TM mode in the x and y directions. While both mode polarizations are free to propagate in the plane, only TM modes have sufficiently large mode index to undergo efficient total internal reflection providing the feedback for lasing.

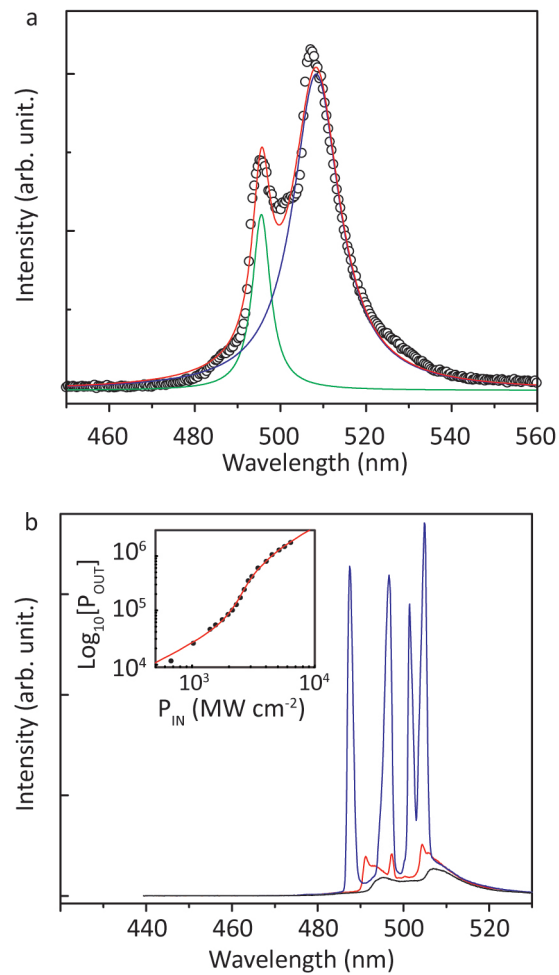


Figure 2 Laser spectra and integrated light-pump response of a room temperature plasmon laser below and above threshold. a The spontaneous emission spectrum at a peak pump intensity of 1960 MW cm^{-2} shows obvious cavity modes albeit being below the threshold which indicates the excellent cavity feedback. **b** room temperature laser spectra and integrated light-pump response (inset) showing the transition from spontaneous emission (1960 MW cm^{-2} , black) via amplified spontaneous emission (2300 MW cm^{-2} , red) to full laser oscillation (3074 MW cm^{-2} , blue).

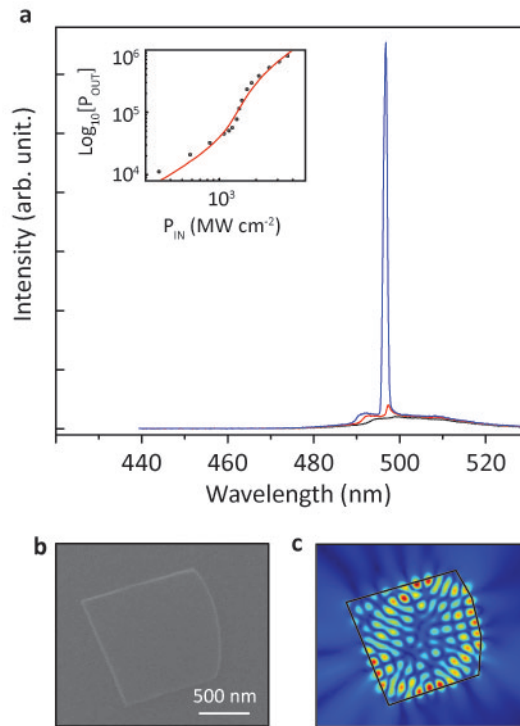


Figure 3 Laser spectrum and integrated light-pump response of a single mode room temperature plasmon laser. **a** The room temperature laser spectra and integrated light-pump response (inset, top) showing the transition from spontaneous emission (1096 MW cm^{-2} , black) via amplified spontaneous emission (1280 MW cm^{-2} , red) to full single mode laser oscillation (1459 MW cm^{-2} , blue) and the spectral narrowing of the single laser mode. **b** shows the SEM micrograph of the device. The curved facet breaks the 4-fold symmetry thereby inhibits high-order modes that exist in the square CdS lasers. **c** shows the electric field intensity distribution of the lasing mode (see supplementary information).

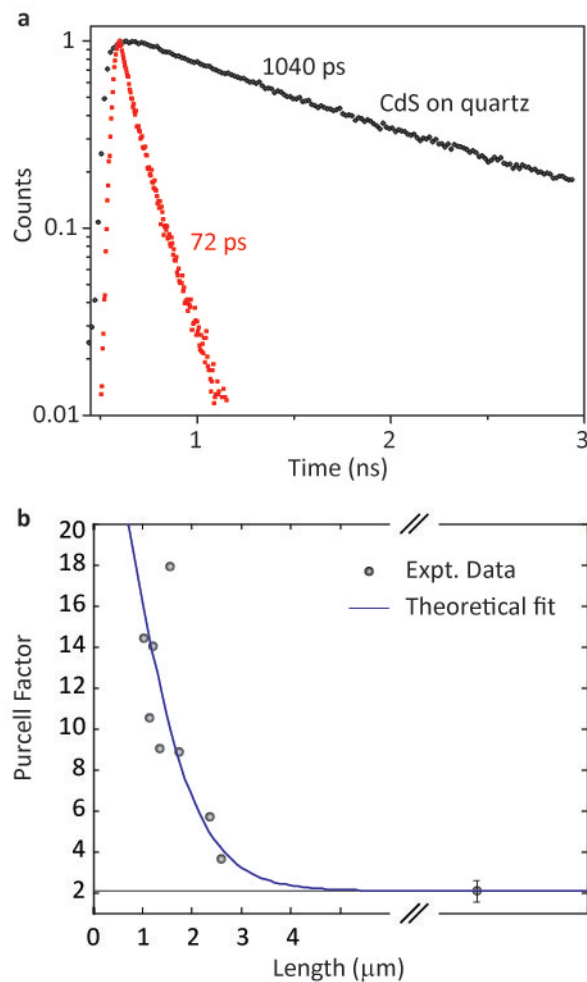


Figure 4 Observation of the Purcell effect. **a** Time resolved spontaneous emission under weak pumping conditions shows a dramatic reduction in lifetime compared with CdS on quartz. The combination of both high cavity quality and strong confinement enhances the spontaneous emission rate by 14 times, due to the Purcell effect [24]. The lifetime is measured for the same device presented in Fig. 1**b**. **b** shows the increase in Purcell effect with the decrease of the cavity side length as a result of the mode volume reduction accompanied by a high quality factor. Very large cavities do not benefit from cavity feedback and exhibit a Purcell effect of 2 due to confinement along the z-direction alone. This agrees well with a simple theoretical model taking into account the numerous emission processes (see Methods). This indicates the ability of these plasmon lasers to strongly enhance light matter interactions. The variations in the CdS thickness (45 to 88 nm) do not play a major role in the emission enhancement.

Methods

Device Fabrication and Experiment Set-up

The CdS squares were made by a solution based sonication cleaving process of CdS nanobelts, which were synthesized via the chemical vapor deposition method [27]. The squares were then deposited from solution on MgF₂/Ag (5 nm/300 nm) substrates. A frequency-doubled, mode-locked Ti-sapphire laser (Spectra Physics) was used to pump the squares ($\lambda_{\text{pump}}=405$ nm, repetition rate 10 KHz, pulse length 100 fs). A 20x objective lens (NA=0.4) focussed the pump beam to ~ 5 μm diameter spot on the sample. All experiments were carried out at room temperature.

Theoretical Purcell Factor

We compare the measured Purcell factors of a number of lasers with a theoretical model in Fig. 4b. For very large cavities, we expect an enhanced emission rate γ_{sp} with respect to the usual rate of CdS band edge transitions, γ_0 , due to strong TM wave confinement. On reducing the cavity size, it can be shown that the feedback increases the emission rate to $\gamma \cong \gamma_{sp} + \bar{Q}B$ where $\bar{Q} = m\pi e^{-\alpha\bar{L}}/(1 - e^{-2\alpha\bar{L}})$ is the averaged cavity mode quality factor; m is the average mode order; α is the round trip cavity loss; \bar{L} is the average round trip path of a TM cavity mode within a CdS square; and B is an unknown factor that depends on the average number of cavity modes and their average mode volume within the CdS emission bandwidth. To facilitate a numerical comparison of this formula with the experimental data, we have derived the basic functional form, $B = \beta L$ and assume that $\bar{L} = L/\sqrt{2}$ is the minimum round trip cavity length (see supplementary information). The Purcell factor, $F = \gamma/\gamma_0 \cong F_\infty[1 + \beta L \text{csch}(\alpha L/\sqrt{2})]$, where F_∞ is the known enhancement factor for large cavities, while α and β are unknowns. The least squares fit in Fig. 4b finds $\alpha = 6,323 \text{ cm}^{-1}$, $\beta = 4.93$, and $F_\infty = 2.08$.